Twistoptics in 1D: Silicon moiré photonic crystals

Tahmid H. Talukdar, Anna Hardison, and Judson D. Ryckman*
Holcombe Department of Electrical and Computer Engineering, Clemson University, Clemson, SC, USA
*jryckma@clemson.edu

2021 IEEE 17th International Conference on Group IV Photonics (GFP) | 978-1-6654-2224-6/21/$31.00 ©2021 IEEE | DOI: 10.1109/GFP51802.2021.9673817

***Abstract*—Analogous to twistronic and twistoptic systems derived from 2D moiré potentials wherein the twist angle is a key parameter, we modulate the 1D moiré pattern in a silicon nanowire and observe lattice mismatch and phase to be critical parameters for controlling photon transport or localization.**

Keywords—integrated optics, photonic crystals, moiré lattices

I. Introduction

Moiré lattices formed by the superposition of two distinctly oriented or sized lattices have recently garnered strong research interest owing to their distinct physics and novel properties. This is exemplified in the recent discoveries associated with the electronic and magnetic properties of 2D atomic materials, i.e. so called 'twistronics', including for example superconductivity in 'magic-twist angle' bilayer graphene, topological valley transport in twisted bilayer superlattices, and the emergence of insulating states and other unconventional band properties [1]. Similarly novel properties and insights into moiré physics are expected to arise from photonic analogues, as explored by Ye's group [2] and other recent works [3]–[5]. Unlike atomic systems, where moiré lattices are generally constrained by the stacking of multiple layers with material specific lattice constants and delicate twist angles, photonic systems offer enormous freedom arising from on-demand patterning with nearly arbitrary lattice dimensions. This makes photonic structures especially well-suited for both investigating moiré physics and harnessing moiré physics in scalable technologies.

II. Design and Modelling

In this work, we superimpose two sub-gratings defined by periods Λ_1 and Λ_2 using two approaches:

(Type A) Asymmetric side-wall modulation: We apply each sub-grating to either side of a sidewall modulated silicon nanowire as illustrated in Fig. 1(a). This structure draws analogy with phase shifted Bragg gratings, and has recently been utilized in specially chirped devices to construct advanced optical filters [6].

(Type B) Symmetric side-wall modulation: We apply each sub-grating to both sides of a sidewall modulated silicon nanowire, superimpose their designs, and perform a Boolean AND operation to define a symmetric moiré grating as illustrated in Fig. 1(b). This design maintains waveguide mirror symmetry and effectively varies the spacing and width of grating teeth. In a separate work, our group has recently employed this grating type to realize quasicrystal interferometers and physical unclonable functions [7].

In analogy to twistronic and twistoptic systems derived from 2D moiré potentials where the twist angle is a key parameter, here we study modulation of the 1D moiré patterns by skewing the sub-lattice mismatch $\Delta\Lambda = \Lambda_2 - \Lambda_1$ (shown below) or initial phase difference ϕ_0 (not shown for brevity). Given two grating periods being Λ_1 and Λ_2, the moiré superperiod is given by $\Lambda_M = 2\Lambda_1\Lambda_2/\Delta\Lambda$ where $\Delta\Lambda$ is the difference between Λ_1 and Λ_2 [6]. In the case where Λ_1/Λ_2 is a rational number, the lattice is deemed commensurable and repeats exactly with a superperiod equal to Λ_M. Otherwise if Λ_1/Λ_2 is irrational the structure is incommensurable and quasi-periodic. The depth of the effective moiré potential then varies with a period equal to $\Lambda_M/2$. As an example, for the choice of periods $\Lambda_1 = 317$ nm and $\Lambda_2 = 318$ nm, the moiré period is $\Lambda_M \approx 200$ µm and the size of a potential well is $\approx$ 100 µm.

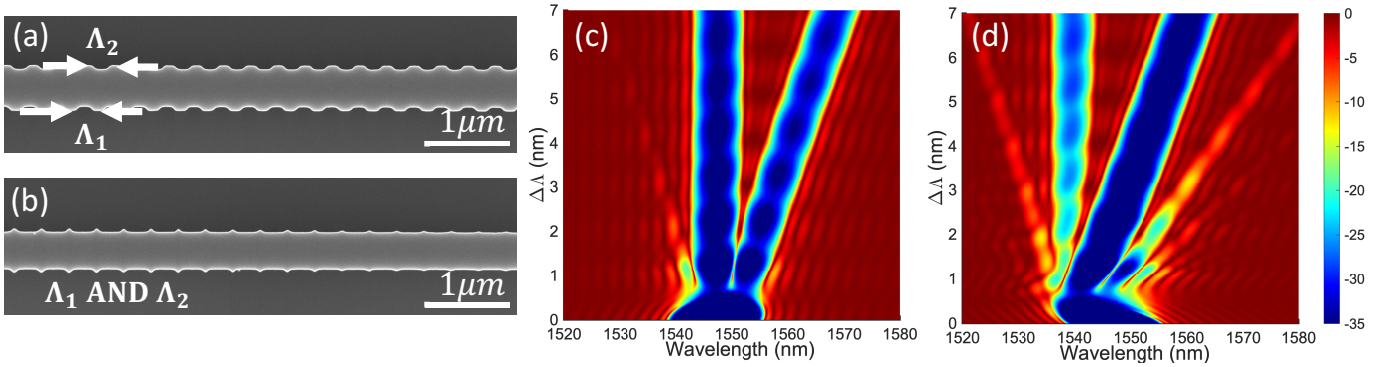

Fig. 1. (Left) SEM images of: (a) type A and (b) type B moiré photonic crystals. (Right) Simulation of waveguide transmission (units: dB) for (c) type A and (d) type B moiré photonic crystals with total length L = 100 μm as a function of wavelength and lattice mismatch $\Delta\Lambda$.

Sponsors: AFOSR FA9550-19-1-0057; NSF CMMI-1825787; (edX UBCx course and SiEPIC support from NSERC).

The optical transmission spectra are modeled using the transfer matrix method as shown in Fig. 1(c & d). As the lattice mismatch is detuned from the conventional Bragg case ($\Delta\Lambda = 0$) to $\Delta\Lambda \approx 0.5$nm, the structure first acts as an apodized grating. Then at $\Delta\Lambda \approx 1$nm a transition occurs wherein cavity resonances are introduced owing to $L > \Lambda_M/2$, i.e. at least one effective moiré potential well fits inside the finite length of the device. For increasing $\Delta\Lambda$ to 2 nm and beyond, the increasing number of cavity modes couple to each other in a cascaded series of nearly identical moiré cavities, effectively forming a special type of coupled-resonator optical waveguide (CROW) [8]. This leads to mini-band formation and anomalously high transmission similar to necklace states, albeit in a non-disordered system. For high Q individual resonators with weak coupling, the dispersion and group velocity of such waveguides can be driven toward zero to realize flatband transport [8], [9].

III. Experiment & Summary

We experimentally validate our model by fabricating the structures on 220 nm device layer SOI platform. Here Λ_1 is kept constant at 317 nm and a period skew is performed on Λ_2 from 317 nm to 324 nm in 0.5 nm intervals to skew $\Delta\Lambda$ from 0 to 7 nm. This is performed for both types A and B. We also experimentally studied the effect of tuning the initial phase ϕ_0 between each sub-lattice (not shown for brevity). The crystal length is fixed to 100 μm, and the fabricated waveguide width is ~460 nm with width modulation of approximately +/- 45 nm.

Figure 2 (a) and 2 (b) show the experimentally measured spectra for type A and B devices, respectively. For design type A in particular, we observe excellent agreement between simulation and experiment. For type B, some of the grating teeth are too small to be fabricated properly leading to increased discrepancies. The red arrow in Fig. 2(a) highlights the fundamental resonance of a moiré photonic crystal cavity. The Q-factor is measured to be near ~25k and is achieved without any systematic design apodization or tapering as in traditional cavities, which is instead provided naturally by the moiré potential. A similar fundamental cavity resonance is identified by the green arrow in Fig. 2(b). The Q-factor in this case is substantially lower, owing to the weaker grating strength of the type B grating. The onset of miniband formation and CROW-like behavior is highlighted in Fig. 2 with the blue arrows.

In summary, we theoretically and experimentally examined moiré photonic structures formed from 1D lattices defined in sidewall modulated silicon photonic nanowires. Unlike certain types of super-periodic systems used to construct optical filters with non-interacting bandgaps, we explored a regime of small lattice mismatches wherein the bandgaps associated with each individual lattice are interacting. This 1D configuration allows us to probe some of the basic, yet nuanced, phenomena associated with wave transport and trapping in super-periodic potentials. At the same time, this work highlights moiré lattices as a promising avenue for continued innovation in integrated optics.

Acknowledgment

We acknowledge the edX UBCx Phot1x Silicon Photonics Design, Fabrication and Data Analysis course organized by Lukas Chrostowski; and Iman Taghavi for performing semi-automated measurements at The University of British Columbia.

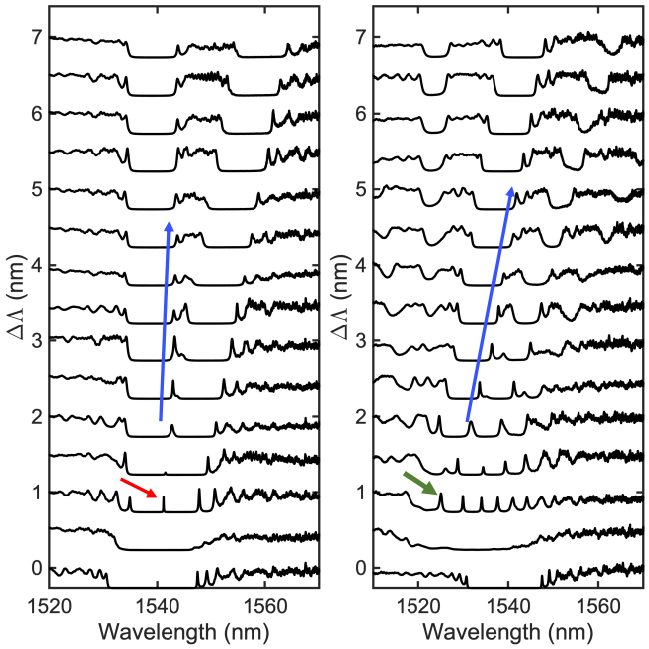

Fig. 2. Experimentally measured transmission spectra for the type A (left) and type B (right) moiré photonic crystals.

References

[1] S. Carr, D. Massatt, S. Fang, P. Cazeaux, M. Luskin, and E. Kaxiras, "Twistronics: Manipulating the electronic properties of two-dimensional layered structures through their twist angle," *Phys. Rev. B*, vol. 95, no. 7, p. 75420, 2017.

[2] P. Wang *et al.*, "Localization and delocalization of light in photonic moiré lattices," *Nature*, vol. 577, no. 7788, pp. 42–46, 2020.

[3] G. Hu, A. Krasnok, Y. Mazor, C. W. Qiu, and A. Alù, "Moiré Hyperbolic Metasurfaces," *Nano Lett.*, vol. 20, no. 5, pp. 3217–3224, 2020.

[4] J. M. Vasiljević, A. Zannotti, D. V. Timotijević, C. Denz, and D. M. J. Savić, "Light propagation in aperiodic photonic lattices created by synthesized Mathieu-Gauss beams," *Appl. Phys. Lett.*, vol. 117, no. 4, 2020.

[5] W. Wang *et al.*, "Moiré Fringe Induced Gauge Field in Photonics," *Phys. Rev. Lett.*, vol. 125, no. 20, p. 203901, 2020.

[6] R. Cheng, N. A. F. Jaeger, and L. Chrostowski, "Fully tailorable integrated-optic resonators based on chirped waveguide Moiré gratings," *Optica*, vol. 7, no. 6, pp. 647–657, 2020.

[7] F. Bin Tarik, A. Famili, Y. Lao, and J. D. Ryckman, "Robust optical physical unclonable function using disordered photonic integrated circuits," *Nanophotonics*, vol. 9, no. 9, pp. 2817–2828, 2020.

[8] A. Yariv, Y. Xu, R. K. Lee, and A. Scherer, "Coupled-resonator optical waveguide : a proposal and analysis," vol. 24, no. 11, pp. 711–713, 1999.

[9] A. G. Yamilov, M. R. Herrera, and M. F. Bertino, "Slow-light effect in dual-periodic photonic lattice," *J. Opt. Soc. Am. B*, vol. 25, no. 4, p. 599, 2008.